THE JOURNAL OF BIOLOGICAL CHEMISTRY VOL. 285, NO. 29, pp. 22676–22688, July 16, 2010
Printed in the U.S.A.

Actin-depolymerizing Factor Cofilin-1 Is Necessary in Maintaining Mature Podocyte Architecture*

Received for publication, March 13, 2010, and in revised form, April 30, 2010 Published, JBC Papers in Press, May 15, 2010, DOI 10.1074/jbc.M110.122929

Puneet Garg[‡], Rakesh Verma[‡], Leslie Cook[‡], Abdul Soofi[‡], Madhusudan Venkatareddy[‡], Britta George[§], Kensaku Mizuno[¶], Christine Gurniak[‖], Walter Witke[‖], and Lawrence B. Holzman[§1]**

*From the [‡]Division of Nephrology, University of Michigan Medical School, Ann Arbor, Michigan 48109, the [§]Department of Veterans Affairs, Philadelphia, Pennsylvania 19104, the [¶]Department of Biomolecular Sciences, Graduate School of Life Sciences, Tohoku University, Sendai, Miyagi 980-8578 Japan, the [‖]Institute of Genetics, University of Bonn, Bonn 53117, Germany, and the **Division of Nephrology, University of Pennsylvania School of Medicine, Philadelphia, Pennsylvania 19104*

Actin dynamics determines podocyte morphology during development and in response to podocyte injury and might be necessary for maintaining normal podocyte morphology. Because podocyte intercellular junction receptor Nephrin plays a role in regulating actin dynamics, and given the described role of cofilin in actin filament polymerization and severing, we hypothesized that cofilin-1 activity is regulated by Nephrin and is necessary in normal podocyte actin dynamics. Nephrin activation induced cofilin dephosphorylation via intermediaries that include phosphatidylinositol 3-kinase, SSH1, 14-3-3, and LIMK in a cell culture model. This Nephrin-induced cofilin activation required a direct interaction between Nephrin and the p85 subunit of phosphatidylinositol 3-kinase. In a similar fashion, cofilin-1 dephosphorylation was observed in a rat model of podocyte injury at a time when foot process spreading is initially observed. To investigate the necessity of cofilin-1 in the glomerulus, podocyte-specific *Cfl1* null mice were generated. *Cfl1* null podocytes developed normally. However, these mice developed persistent proteinuria by 3 months of age, although they did not exhibit foot process spreading until 8 months, when the rate of urinary protein excretion became more exaggerated. In a mouse model of podocyte injury, protamine sulfate perfusion of the *Cfl1* mutant mouse induced a broadened and flattened foot process morphology that was distinct from that observed following perfusion of control kidneys, and mutant podocytes did not recover normal structure following additional perfusion with heparin sulfate. We conclude that cofilin-1 is necessary for maintenance of normal podocyte architecture and for actin structural changes that occur during induction and recovery from podocyte injury.

Glomerular visceral epithelial cells or podocytes play a central role in maintaining the selective filtration barrier of the kidney that prevents the passage of cellular elements and large macromolecules from the blood into the urinary space. Podocytes are unique cells with interdigitating foot-like actin-rich processes that arise from their cell bodies and surround glomerular capillary walls. An ultrafiltrate of serum passes across this specialized intercellular junction, also termed the *slit diaphragm*, formed at the interface of these interdigitating foot processes.

There appears to be a direct relationship between the integrity of the podocyte intercellular junction and the three-dimensional architecture of the podocyte. When injured, podocytes undergo a dramatic change in their morphology termed *foot process effacement* that appears to result from incompletely understood alterations in cytoskeletal and intercellular junctional architecture. Foot process effacement is a dynamic and reversible process that correlates with the development of proteinuria both in human disease and in experimental models. Recent investigations have demonstrated a functional relationship between molecular components of the foot process intercellular junction and actin dynamics. The importance of these relationships is emphasized by human genetic mutations in actin associated proteins that result in foot process effacement and proteinuria (1–6).

Cofilin is a ubiquitous actin-binding protein that is essential for actin filament elongation and remodeling. Cofilin activity severs existing actin filaments, resulting in creation of new filament fragments with both barbed (+) and pointed ends (−). Subsequently, rapid polymerization can occur at the newly created barbed ends (7–9). Cofilin also disassembles actin monomers from the pointed end (−) of the actin filament, which is then recycled to the barbed end (10, 11). Given these functions, cofilin is necessary for directed motility, cell division, and the establishment of polarity in cultured cells (12–15). Phosphorylation of cofilin on serine 3 results in reduced actin binding and depolymerizing activity. Several signal transduction pathways that cause actin reorganization also induce rapid dephosphorylation of cofilin (16–18). Phosphorylation of cofilin on its Ser[3] residue is mediated by LIM kinases (LIMKs)[2] (Lin-11/Isl-1/Mec-3 kinases) LIMK1 or LIMK2 (19, 20) and by testicular protein kinases (13, 21). Two phosphatases, slingshot (SSH)

* This work was supported, in whole or in part, by National Institutes of Health Grant DK081403 (to P. G.). This work was also supported by American Recovery and Reinvestment Act supplement DK081403-02W1 (to L. B. H.), a Veterans Affairs Merit Review (to L. B. H.), and a National Kidney Foundation Young Investigator Award (to P. G.).

[1] To whom correspondence should be addressed: 410E Hill Pavilion, 380 S. University Ave., Philadelphia, PA 19104. Tel.: 215-583-1840; E-mail: lholzman@upenn.edu.

[2] The abbreviations used are: LIMK, LIM kinase; MES, 2-(*N*-morpholino)ethanesulfonic acid; ADF, actin-depolymerizing factor; GST, glutathione *S*-transferase; HA, hemagglutinin; GFP, green fluorescent protein; PBS, phosphate-buffered saline; CD, cytoplasmic domain; HBSS, Hanks' balanced salt solution; shRNA, short hairpin RNA; PAN, puromycin aminonucleoside.

and chronophin, have been implicated in dephosphorylation of the cofilin Ser[3] residue, which activates cofilin (12, 22).

Nephrin is a transmembrane protein of the immunoglobulin superfamily that is targeted to the podocyte intercellular junction. The absence or inherited mutation of Nephrin results in proteinuria and abnormality of foot process development. Engagement of the Nephrin extracellular domain results in Src family kinase Fyn-dependent tyrosine phosphorylation of the Nephrin cytoplasmic domain and subsequent recruitment of Src homology 2 domain adaptor proteins, including Nck1/2, phospholipase Cγ, and the p85 subunit of PI3K (23–26). Nephrin-dependent signal transduction appears to regulate actin dynamics because Nephrin recruits components of the actin polymerization complex, including Arp2/3 complex and N-WASP, synaptopodin, ZO-1, IQGAP1, and CD2ap (27–29), and Nephrin activation can induce actin filament nucleation and elongation (23, 24).

During podocyte development, cuboidal cells send out processes that ultimately interdigitate and form the specialized podocyte intercellular junction. Presumably, podocyte process formation requires a highly regulated dynamic of actin polymerization and remodeling. Similar events must also occur during podocyte effacement and subsequent repair. Based on these observations, we hypothesized that regulation of cofilin activity might play an important role in podocyte development and function.

EXPERIMENTAL PROCEDURES

Antibodies—Purified rabbit polyclonal antibodies against Nephrin (30) and phospho-Nephrin (23) were described previously. Antibodies against cofilin, phosphocofilin, LIMK, and phospho-LIMK1(Thr[508]) were obtained from Cell Signal. CD16 (clone 3G8) antibody (Beckman Coulter), rhodamine-conjugated goat anti-mouse IgG (Pierce), anti-SSH1 antibody (Bethyl Laboratories), p85 (Cell Signaling), actin-depolymerizing factor (ADF), GST-horseradish peroxidase, and FLAG antibodies (Sigma) were obtained commercially. 50A9 antibody was a gift from K. Tryggvason (31). Phospho-SSH1 (phospho-Ser[978]) antibody was prepared as reported previously (12, 32). Cofilin-1 (ECM Bioscience), cofilin-2 (Upstate), anti-Myc, and HA (Invitrogen) antibodies were also obtained commercially.

Plasmids—Plasmid encoding GFP-cofilin and LIMK was a gift from Gary Bokoch (Scripps Research Institute, La Jolla, CA), and plasmid encoding HA-14-3-3ζ was a gift from B. Margolis (University of Michigan, Ann Arbor, MI). Slingshot plasmids, including catalytic dead, single, and compound mutations, were prepared as reported previously (12). Mammalian plasmids encoding mouse Nephrin (30), Fyn (33), Fyn KD (K295M), and human Nephrin (gift from K. Tryggvason) (31) were described previously. The CD16-HA (containing an HA tag) construct was a gift from B. Mayer (University of Connecticut) (34). Constructs encoding fusion protein consisting of CD16 extracellular domain, CD7 transmembrane domain, and Nephrin cytoplasmic domain and their mutants were generated using PCR-based techniques and described previously (23, 35). Restriction digestion and DNA sequencing were used to confirm all construct sequences. Slingshot was cloned into Ds-Red plasmid (Clontech) using a standard PCR method and Clontech in-fusion technology.

Immunoprecipitation and Immunoblotting—Proteins were extracted from plasma membranes in radioimmune precipitation buffer (PBS containing 0.1% SDS, 1% Nonidet P-40, 0.5% sodium deoxycholate, and 100 mM potassium iodide). Endogenous immunoprecipitation were performed by extracting tissue in radioimmune precipitation buffer containing 0.1% bovine serum albumin.

Cell Culture—Transient transfections were carried out in human podocyte cells (gift from Moin Saleem) (36) cultured in RPMI with Glutamax (Invitrogen) supplemented with 10% fetal bovine serum (Invitrogen) and 200 units/ml penicillin and streptomycin (Roche Applied Science) along with ITS (insulin, transferrin, and selenium) (Invitrogen). Transfections were performed using Lipofectamine 2000 (Invitrogen) and electroporation using an Amaxa Nucleofactor II (Amaxa Biosystems) as per the manufacturer's directions. The maintenance of HEK293 cells stably expressing human Nephrin was described previously (23). The mouse podocyte immortalized cell line (a gift from Karl Endlich) (37) has been described previously. For 50A9 antibody studies, HEK293 cells stably expressing human Nephrin were serum-starved for 30 min prior to treatment with monoclonal antibody 50A9 (10 μg/ml) in complete media and incubated for 30 min at 4 °C. Cells were washed and treated with anti-mouse IgG (20 μg/ml) for 5 min at 37 °C and lysed in radioimmune precipitation buffer. In experiments using PI3K or phospholipase C inhibitors, cells were incubated with 100 nM wortmannin, 10 μM LY294002, or 10 μM U73122 (Sigma) for 30 min prior to clustering. The C2C12 mouse myoblast cell line was obtained from ATCC.

Puromycin Aminonucleoside Nephrosis—Female Sprague-Dawley rats weighing 200–250 g were injected with puromycin aminonucleoside (Sigma) (10 mg/100 g) or PBS (vehicle) intraperitoneally. Rats were sacrificed, and glomeruli were isolated using graded sieving as described previously (29).

Pull-down—Recombinant GST and His fusion proteins were prepared and purified from BL21 *Escherichia coli*. Where indicated, tyrosine-phosphorylated His-Nephrin cytoplasmic domain (CD) was expressed in and purified from TKB1 *E. coli* cells (Stratagene). Purified His tag proteins bound to Talon® magnetic beads (Invitrogen) were incubated with purified GST recombinant proteins where indicated. After washing with PBS containing 0.1% Tween 20, 1 mM sodium orthovanadate, and 1 mM sodium fluoride, protein complexes were eluted. Eluate was resolved by SDS-PAGE in replicates prior to immunoblotting with the indicated antibodies.

CD16/CD7/Neph1 Chimera and Cofilin Recruitment Experiments—Human podocyte cells were transfected with CD16/CD7 chimeric constructs bearing HA, Nephrin CD, and various mutants at the C-terminal end. Thirty hours following transfection, RPMI medium was removed and replaced with fresh medium containing 1 μg/ml CD16 antibody (clone 3G8, Beckman Coulter). Cells were maintained on ice for 1 h. At this point, cells were washed twice with PBS, 1 μg/ml rhodamine-conjugated or unlabeled anti-mouse IgG (Pierce) was added to the media, and incubation was continued at 37 °C for 30 min. Cells for immunofluorescence were washed three times with

TABLE 1
shRNA sequence for knockdown of human slingshot and cofilin

shRNA	Sequence
SSH1 shRNA 1	CCGGCGGCACACGTTCTAGCTCATTCTCGAGAATGAGCTAGAACGTGTGCCGTTTTT
SSH1 shRNA 2	CCGGCATCTTTATCTCGGCTCTGAACTCGAGTTCAGAGCCGAGATAAAGATGTTTTT
SSH1 shRNA 3	CCGGGCTGTCTGAGTATGAAGGCATCTCGAGATGCCTTCATACTCAGACAGCTTTTT
SSH1 shRNA 4	CCGGTGAGGATGAAACTGGCAGCTTCTCGAGAAGCTGCCAGTTTCATCCTCATTTTT
Cfl1 shRNA 1	CCGGCTATGAGACCAAGGAGAGCAACTCGAGTTGCTCTCCTTGGTCTCATAGTTTTT
Cfl1 shRNA 2	CCGGCTGACAGGGATCAAGCATGAACTCGAGTTCATGCTTGATCCCTGTCAGTTTTT
Cfl1 shRNA 3	CCGGGCCCTCTATGATGCAACCTATCTCGAGATAGGTTGCATCATAGAGGGCTTTTT
Cfl1 shRNA 4	CCGGCCAGATAAGGACTGCCGCTATCTCGAGATAGCGGCAGTCCTTATCTGGTTTTT
Cfl1 shRNA 5	CCGGCAAGCATGAATTGCAAGCAAACTCGAGTTTGCTTGCAATTCATGCTTGTTTTT

PBS and fixed with cytoskeleton buffer. The composition of cytoskeleton buffer stock was 10 mM MES, 138 mM KCl, 3 mM $MgCl_2$, 2 mM EGTA, and sucrose to a final concentration of 0.32 M. On the day of use, 20% paraformaldehyde was added to cytoskeleton buffer stock to achieve a final concentration of 4%. Coverslips were mounted on glass slides using ProLong Gold antifade reagent (Invitrogen). Samples were analyzed by fluorescence confocal microscopy with an Olympus FV-500 microscope using a ×100 oil immersion objective lens and Fluoview software (version TIEMPO 4.3; Olympus). Images were processed using Adobe Photoshop software. All images were acquired at 1024 × 1024-pixel resolution.

Cofilin-1 flox Mice—Cofilin-1 flox mice were a kind gift from Walter Witke (EMBL, Italy) (14, 38). We bred the cofilin flox $Cfl1^{\Delta E2/\Delta E2}$ mouse with the podocin promoter-driven Cre *NPHS2-Cre*$^{+/+}$ mouse described before (39, 40). Mice homozygous for the *flox* allele having a *Cre* allele were used for the experiments. Their littermates homozygous for the *flox* allele but lacking the *Cre* allele were used as controls. All animal experiments were approved by the University Committee on the Use and Care of Animals Institutional Review Board at the University of Michigan Medical School. The urine albumin/creatinine ratio was determined from urine obtained in metabolic cages by direct competitive enzyme-linked immunosorbent assay for urine albumin (Nephrat II, Exocell, Inc.) and Jaffé reaction for urine creatinine (Creatinine Companion, Exocell, Inc.). Mice were sacrificed, and kidneys were isolated. Sections of the kidneys were processed for electron microscopy, histopathology, and immunofluorescence.

Mouse Kidney Perfusion—Perfusion of mouse kidneys with protamine sulfate was carried out as described previously (23, 41). Briefly, 3-month-old $Cfl1^{fl/fl}$ (control) and littermate $Cfl1^{\Delta E2/\Delta E2}$ (null) mice were anesthetized with pentobarbital; mouse core temperature was monitored with a rectal probe, and animals were maintained at 37 °C throughout the procedure using a heating pad apparatus. Kidneys were perfused with solutions maintained at 37 °C through the left ventricle at a pressure of ~70 mm Hg and an infusion rate of 10 ml/min (42). Perfusion was carried out with HBSS for 2 min, followed by perfusion with protamine sulfate (2 mg/ml in HBSS; Sigma) for 15 min. For effacement recovery, following perfusion with protamine sulfate, mice were perfused with heparin sulfate (800 μg/ml in HBSS; Sigma) for 15 min (41). Kidneys were fixed by perfusion with 3% paraformaldehyde in PBS before further processing for transmission electron microscopy or indirect immunofluorescence microscopy. All animal experiments were approved by the University Committee on the Use and Care of Animals Institutional Review Board at the University of Michigan Medical School. All work was conducted in accord with the principles and procedures outlined in the National Institutes of Health Guidelines for the Care and Use of Experimental Animals.

Indirect Immunofluorescence Microscopy—Adult or newborn mouse kidney was fixed in 4% paraformaldehyde and paraffin-embedded. Sections (4 μm) were cut, deparaffinized in xylene, and rehydrated through graded alcohols in H_2O. Epitope retrieval was achieved by heating sections at 98 °C for 2 h in Retrieve-All-1 (1×; Signet Laboratories Inc.). Sections were cooled to room temperature for 10 min, rinsed with water for 1 min, placed in 1× PBS for 5 min, and made permeable by incubating with 1% SDS in PBS for 10 min. Sections were blocked for 20 min in 10% goat serum prior to overnight incubation of primary antibodies at 4 °C. After three washes, secondary antibodies were added at room temperature for 60 min. Slides were washed and mounted with a coverslip using ProLong Antifade mounting medium (Invitrogen). Immunofluorescence images were obtained with a Leica DMIRB inverted microscope and an RT slider digital camera (model 2.3.1; Diagnostic Instruments) and collected with SPOT software (version 4.5; Diagnostic Instruments) and prepared for presentation with Adobe Photoshop CS4.

Electron Microscopy—Preparation of samples for transmission electron microscopy was performed by standard methods using pieces of diced kidney perfusion fixed in glutaraldehyde/cacodylate buffer. After plastic embedding, 1-μm sections were cut and stained with toluidine blue. Selected samples containing glomeruli were thin-sectioned and examined by transmission and scanning electron microscopy (42). Twenty glomeruli from each kidney were examined before representative images were chosen.

SSH1 and CFL1 Stable Knockdown Podocyte Cell Line—We generated human podocyte cell lines with stable knockdown of SSH1 and cofilin-1 using four or more different prepackaged lentivirus-based shRNA oligonucleotides from Sigma (Mission shRNA Lentiviral Transduction Particles). The sequences of the different shRNAs are shown in Table 1. Following infection of human podocytes using Polybrene, cells with stable integration were selected using puromycin. Knockdown of protein expression was confirmed by Western blot.

Podocyte Cell Count and Slit Diaphragm Frequency Analysis—Podocyte cell count and slit diaphragm frequency analysis were done as described previously by Wiggins *et al.* (43, 44). In brief, 3-μm-thick kidney sections from control and *Cfl1* null mice were stained with monoclonal WT1 antibody (Santa Cruz

Biotechnology, Inc., Santa Cruz, CA). Cy3-conjugated goat anti-mouse IgG (Jackson ImmunoResearch Laboratories, West Grove, PA) was used as a secondary antibody to fluorescently label WT1 protein. Glomerular volume data were obtained from 50 consecutive 3-μm glomerular cross-sections photographed (Leica Microsystems) at $\times$20 magnification by systematically moving from top to bottom in an "S" shape fashion, and images were stored digitally for analysis. The area of every glomerular profile was measured manually by tracing the glomerular outline on a computer screen and calculating the area by computerized morphometry with the Metamorph Image System (Metamorph, Universal Imaging, Downington, PA). The average glomerular tuft volume was calculated using the Weibel formula as described previously (45), representing the mean value determined from 50 consecutive glomerular tuft cross-sections. WT1-positive nuclei were identified by immunofluorescence staining. The estimate of the average number of podocytes per glomerulus was determined by the stereological method of particle density proposed by Weibel (45, 46).

To assess slit frequency quantitatively, transmission electron micrographs of kidneys from *Cfl1*$^{fl/fl}$ (control) and *Cfl1*$^{\Delta E2/\Delta E2}$ (null) were used. The number of intercellular junctions per 5-μm length of GBM was counted using the ImageJ software (National Institutes of Health) in regions adjacent to the urinary space.

RESULTS

Nephrin Interacts with Cofilin-1 in Podocytes—Cofilin exists in three isoforms in eukaryotes named cofilin-1 (also called cofilin-n), cofilin-2 (cofilin-m), and ADF; cofilin-1 is predominantly expressed in non-muscle cells, and cofilin-2 is expressed in muscle cells. In initial experiments, we observed that cofilin-1 and ADF but not cofilin-2 are expressed in cultured human and mouse podocytes (Fig. 1*A*). Because Nephrin activation has been implicated in regulating actin dynamics, the interaction of endogenous cofilin-1 and Nephrin was investigated by co-immunoprecipitation from rat isolated glomerular lysate. Cofilin co-immunoprecipitated readily with Nephrin under the conditions described (Fig. 1*B*). This interaction appeared to be indirect because an interaction between Nephrin and cofilin-1 protein was not observed when these purified recombinant proteins were combined *in vitro* and co-immunoprecipitated (data not shown).

Nephrin Engagement Results in Cofilin-1 Dephosphorylation—We hypothesized that Nephrin engagement would result in cofilin-1 activation. As described previously (Fig. 1*C*), a series of chimeric protein expression constructs were created in which a CD16 extracellular domain and a CD7 transmembrane domain were coupled to either the Nephrin cytoplasmic domain (CD16-Nephrin) or to mutant Nephrin cytoplasmic domains (20, 39). These fusion proteins were expressed in a human podocyte cell line. After the addition of mouse anti-CD16 antibody and a secondary anti-mouse IgG antibody to the culture medium of live cells, "clustering" of CD16/CD7 fusion proteins on the plasma membrane was readily visualized (Fig. 1*D*; additional control data not shown). To test the possibility that clustering of the Nephrin cytoplasmic domain results in the recruitment of cofilin-1, human podocytes were co-transfected with plasmid encoding CD16-Nephrin and cofilin-1-GFP and were examined by immunofluorescence confocal microscopy. In the presence of aggregating antibody, cofilin-1-GFP co-localized at the plasma membrane in clusters with CD16-Nephrin (Fig. 1*D*). Simultaneously, we observed marked cofilin Ser^3 dephosphorylation by 30 min following the addition of clustering antibody (Fig. 2*A*). By an alternative approach, HEK293 cells stably expressing full-length human Nephrin were transfected with cofilin-1-GFP. An activating anti-human Nephrin extracellular domain monoclonal antibody (50A9) (31) or control antibody was added to culture medium prior to cell lysis. In co-immunoprecipitation experiments, Nephrin and cofilin-1-GFP interacted independently of the addition of 50A9 antibody. Like the results obtained after clustering CD16-Nephrin, cofilin-1(Ser^3) phosphorylation was decreased when Nephrin was activated using 50A9 antibody (Fig. 1*E*). These observations provided preliminary evidence that Nephrin engagement might participate in regulating cofilin-1 activity and actin remodeling because dephosphorylation of cofilin Ser^3 correlates with increased cofilin-dependent actin depolymerizing activity.

To examine this phenomenon in an *in vivo* model, cofilin Ser^3 phosphorylation was examined in the puromycin aminonucleoside (PAN) rat model of podocyte injury, a model that we have characterized previously (35). Three days after injury induction, cofilin Ser^3 phosphorylation was remarkably attenuated in glomerular lysates obtained from rats treated with PAN compared with control (Fig. 1*F*), suggesting that cofilin-1 is activated in response to glomerular injury.

Nephrin Interacts with PI3K—The signaling mechanism by which cofilin is activated by other plasma membrane receptors is complex and has been described (12, 25, 47). We examined whether Nephrin-induced cofilin dephosphorylation employs a signaling mechanism similar to that employed in these systems where cofilin dephosphorylation is dependent on the activity of the cofilin phosphatase Slingshot, the activity of an unknown Slingshot phosphatase, and PI3K activity. Because others have shown that Nephrin interacts (at least indirectly) with the p85 regulatory subunit of PI3K (26), we employed the CD16-Nephrin model described above to examine whether Nephrin-induced cofilin dephosphorylation is PI3K-requiring. In this model, CD16-Nephrin activation-induced cofilin dephosphorylation was PI3K-dependent because the addition of PI3K inhibitors blocked Nephrin activation-induced cofilin Ser^3 dephosphorylation (Fig. 2*A*).

The direct interaction of Nephrin with p85 was confirmed *in vitro* using purified recombinant proteins (Fig. 2*B*). To obtain tyrosine-phosphorylated Nephrin, His-tagged Nephrin was expressed in TKB1 *E. coli* containing a tyrosine kinase that promiscuously catalyzes the phosphorylation of tyrosine residues on the expressed protein or in BL21 *E. coli* that do not contain this kinase activity. Purified phosphorylated or unphosphorylated His-tagged Nephrin was mixed with GST-p85. Nephrin and p85 co-immunoprecipitated only when Nephrin was tyrosine-phosphorylated in this system. The interactions with Nephrin of several Src homology 2 domain-containing adaptor proteins were found previously to be Fyn-requiring (Nck (23, 24), Crk (25), and phospholipase γ (25)). Therefore, it was not surprising that ectopic expression of Fyn augmented the

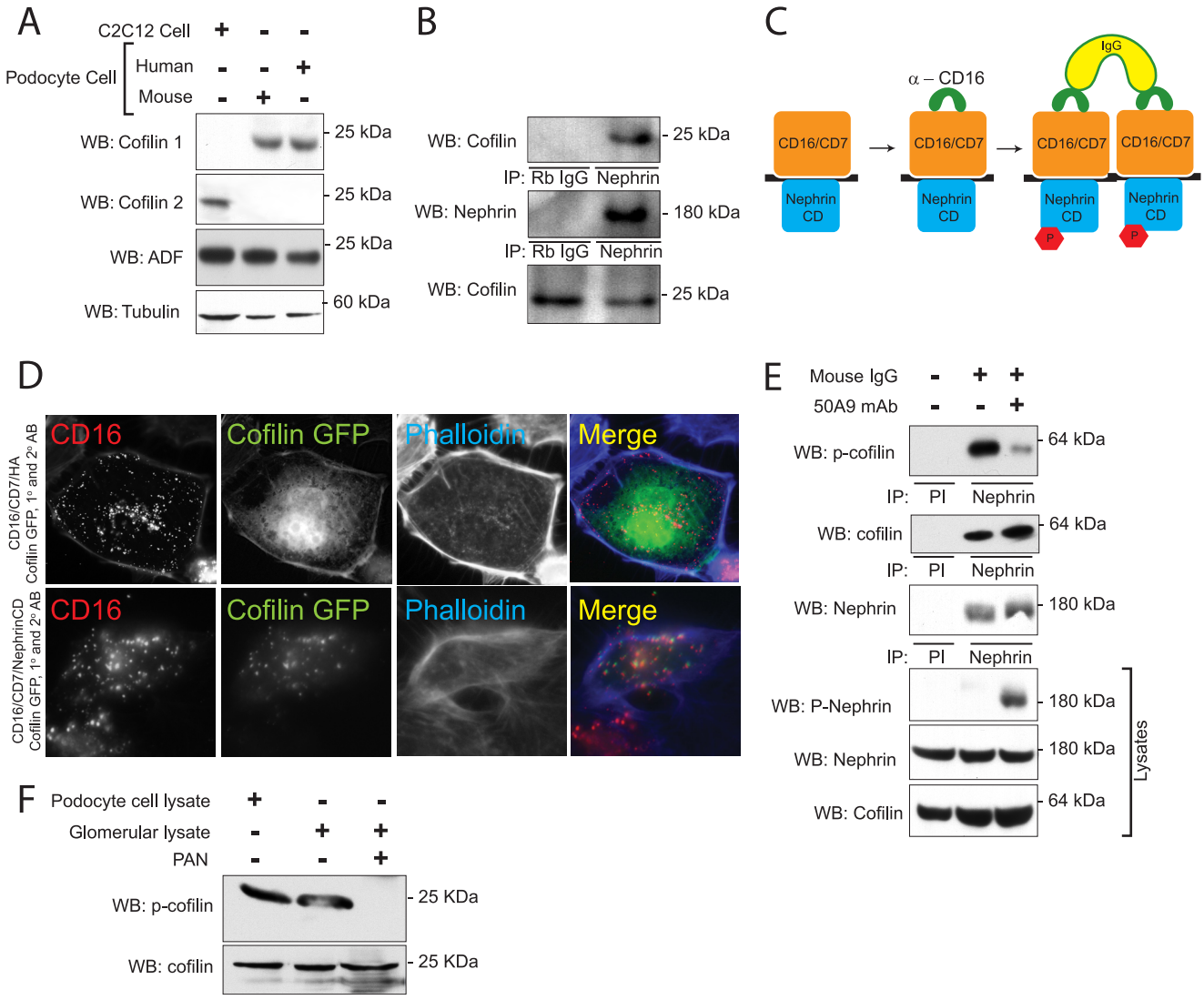

FIGURE 1. **Cofilin-1 is expressed in podocytes and interacts with Nephrin.** *A*, expression of cofilin and its isoforms in cultured podocytes. Cell lysates from human and mouse podocyte immortalized cell lines were blotted with cofilin-1, cofilin-2, and ADF isoform-specific antibodies. Lysate from myoblast cell line was used as a positive control for cofilin-2. *B*, Nephrin and cofilin associate in vivo. Co-immunoprecipitation experiments performed on mouse glomerular lysate using antibodies against Nephrin and cofilin. *C*, schematic showing the CD16 clustering system. Chimeras with CD16 extracellular domain, CD7 transmembrane domain, and Nephrin cytosplasmic domain are clustered by the addition of anti-CD16 antibody and subsequently anti-mouse IgG, resulting in phosphorylation of Nephrin tyrosine residues. *D*, cofilin is recruited to the CD16/CD7/Nephrin CD cluster at the plasma membrane. Human podocytes expressing indicated CD16/CD7 chimeric proteins (*red*) and GFP-cofilin (*green*) were treated with anti-CD16 antibody (primary) and rhodamine-conjugated anti-IgG antibody (secondary) and then fixed and examined by confocal microscopy. CD16-HA represents a CD16/7 chimera in which the Nephrin cytoplasmic domain is replaced by an HA tag and serves as control. Data are representative of three separate experiments. Magnification was ×600. *E*, HEK293 cells expressing full-length human Nephrin and GFP-cofilin-1 were treated with 50A9 anti-Nephrin antibody followed by anti-mouse IgG. Lysates were immunoprecipitated with anti-Nephrin antibody and immunoblotted for phosphocofilin(phospho-Ser[3]). *F*, serine 3 phosphorylation of cofilin is attenuated in the PAN-induced podocyte injury model. Glomerular lysates from rats injected with PBS (control) or PAN were lysed and immunoblotted as shown. Immortalized human podocyte cell lysate were immunoblotted for the presence of cofilin and phosphocofilin as control. *WB*, Western blot; *IP*, immunoprecipitation; *PI*, preimmune serum.

affinity of the interaction between Nephrin and p85 when Nephrin and p85 were co-expressed with Fyn in human podocyte cell culture, recapitulating earlier published results (Fig. 2*C*) (26).

Mouse Nephrin cytoplasmic domain residues Tyr^2 and Tyr^3 (see Table 2) were previously reported to be necessary for the Nephrin-p85 PI3K interaction (26). In initial experiments using CD16 Nephrin chimeras with Tyr^2 and Tyr^3 single and compound mutations, we were unable to completely abrogate cofilin dephosphorylation on clustering. This suggested the possibility that additional tyrosine residues might be involved in mediating the Nephrin-PI3K interaction. To re-examine the Nephrin motifs involved in this interaction, 11–18-mer oligopeptides were synthesized encompassing each tyrosine residue within the Nephrin cytoplasmic domain and in which the tyrosine residue was either phosphorylated or not phosphorylated (Sigma Genosys PEPScreen®) (Table 2). Using these peptides, an overlay experiment was performed to examine the affinity of p85 PI3K for these peptides. Under these conditions, we observed binding of GST-p85 to the peptide spanning the Nephrin Tyr^1 (see Table 2) residue and to the previously described Tyr^2 residue (Fig. 3*A*).

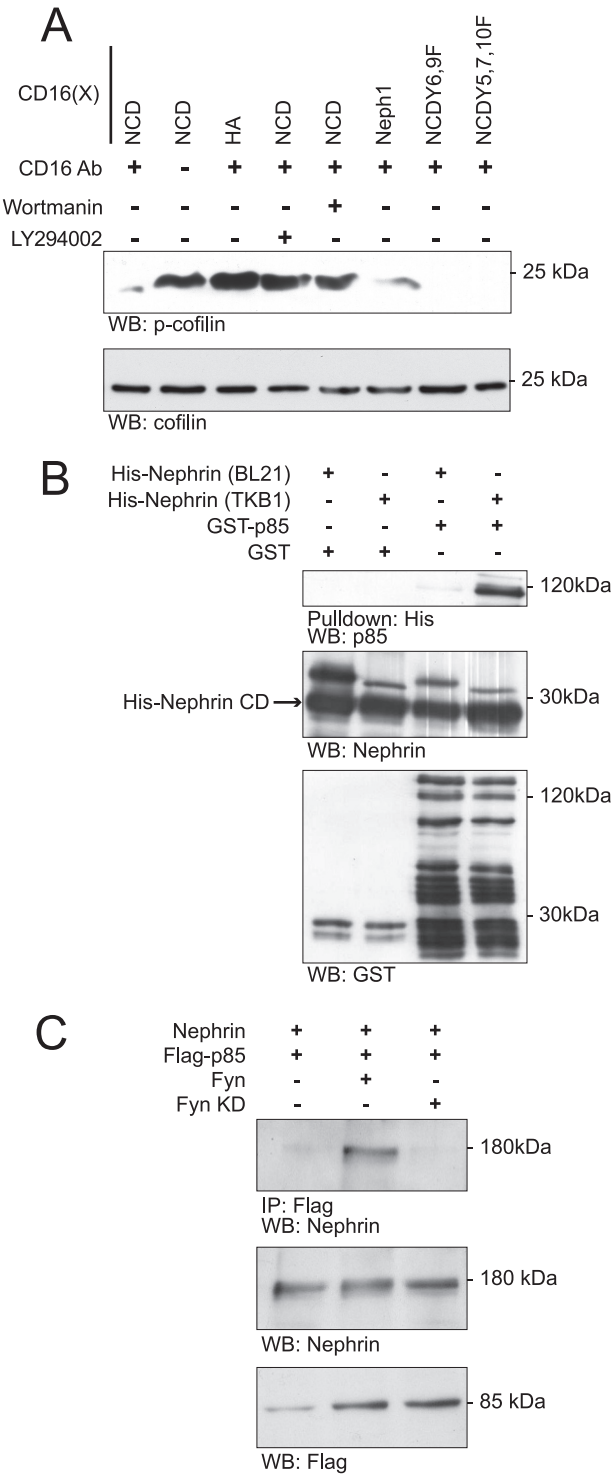

FIGURE 2. **Nephrin interacts with the p85 subunit of PI3K.** *A*, Nephrin-mediated cofilin Ser^3 dephosphorylation is abrogated by PI3K inhibitors. Human podocytes expressing indicated CD16-Nephrin cytoplasmic domain (*CD16-NCD*) or CD16-Neph1 cytoplasmic domain (*CD16-Neph1*) plasmids were pretreated with LY294002 and wortmannin before chimeric proteins were clustered and activated with anti-CD16 antibody and secondary antibody. CD16-NCD plasmids with the indicated tyrosine to phenylalanine mutations were used as controls because mutations at these sites were shown previously to interact with Src homology 2 domain adaptor proteins other than the p85 subunit of PI3K. Lysates from the experiment were divided into two equal samples and loaded on two separate gels. *B*, direct interaction between Nephrin and PI3K p85 subunit. Purified recombinant His-Nephrin cytoplasmic domain expressed in BL21 or TKB1 *E. coli* and GST-p85 were mixed and pulled down using cobalt-conjugated magnetic beads (Talon®, Invitrogen) and then immunoblotted with anti-p85 antibody. Control immunoblots demonstrate the presence of recombinant Nephrin, GST, and GST-p85. *C*, Nephrin interacts with p85 only in the presence of Fyn. Human podocytes expressing the indicated plasmids were lysed and immunoprecipitated with FLAG antibody and then blotted with Nephrin antibody. Lysates were also blotted to detect expression of Nephrin or FLAG-p85. Kinase-dead Fyn (*Fyn KD*) was used as a negative control. *WB*, Western blot; *IP*, immunoprecipitation; *p-cofilin*, phosphocofilin. Data are representative of four experiments.

TABLE 2
Tyrosine residues of mouse nephrin cytosplamsic domain

Residue	Sequence	Alternate tyrosine number used throughout
Tyr^{1128}	YEES	Tyr^1
Tyr^{1153}	YYSN	Tyr^2
Tyr^{1154}	YYSN	Tyr^3
Tyr^{1172}	YRQA	Tyr^4
Tyr^{1191}	YDEV	Tyr^5
Tyr^{1198}	YGPP	Tyr^6
Tyr^{1208}	YDEV	Tyr^7
Tyr^{1216}	YDLR	Tyr^8
Tyr^{1225}	YEDP	Tyr^9
Tyr^{1232}	YQDV	Tyr^{10}

Nephrin Engagement Results in Slingshot and LIMK1 Dephosphosphorylation—The phosphatases SSH and chronophin dephosphorylate and activate cofilin. In a proximal event described previously, 14-3-3 appears to regulate SSH activity by binding SSH1 when SSH1 is phosphorylated on residues Ser^{937}/Ser^{978} (12, 32). Dephosphorylation of the Ser^{978} residue decreases the affinity of 14-3-3 for SSH1, resulting in the release of SSH, SSH translocation to the leading edge, and SSH activation. We examined whether Nephrin activation would induce similar changes (Fig. 3). In preparation for this set of experiments, cultured human podocytes were stably depleted of SSH1 by RNA interference ($SSH1^{kd}$). Optimal knockdown of SSH1 was obtained using shRNA (clone 1) (Fig. 3*B*) containing a sequence identical to one found in the 3′-untranslated region of the *SSH1* gene. In rescue experiments, wild type SSH1 was expressed in $SSH1^{kd}$ cells by transient transfection. In this system, CD16-Nephrin clustering induced SSH1 Ser^{978} dephosphorylation, an event that required Nephrin tyrosine residues Tyr^1 and Tyr^2 (Fig. 3*C*), implying that Nephrin-induced PI3K activation is necessary for SSH1 dephosphorylation. That application of PI3K inhibitor wortmannin and LY294002 also inhibited SSH1 dephosphorylation in this model is consistent with this observation. As anticipated, Nephrin activation also induced decreased affinity of SSH1 and 14-3-3 in this system, an effect that was attenuated when Nephrin (Y2F/Y3F) was introduced (Fig. 3*D*). This system was also used to test the necessity of SSH1 in Nephrin activation-induced cofilin dephosphorylation and the necessity of phosphorylation of SSH1 (Ser^{937}, Ser^{978}) in this process. Nephrin-activated dephosphorylation of cofilin was observed when $SSH1^{kd}$ cells were rescued with wild type SSH1 or SSH1 (S937A/S978A) mutants (*SSH1(2SA)*) (Fig. 3*E*). Nephrin activation did not result in cofilin dephosphorylation when SSH1(CS) (a phosphatase-dead mutant with a cysteine to serine mutation in its catalytic pocket) was substituted for wild type SSH1. These results are consistent with the observation that Nephrin activation-induced cofilin dephosphorylation requires SSH1 and Ser^{978}.

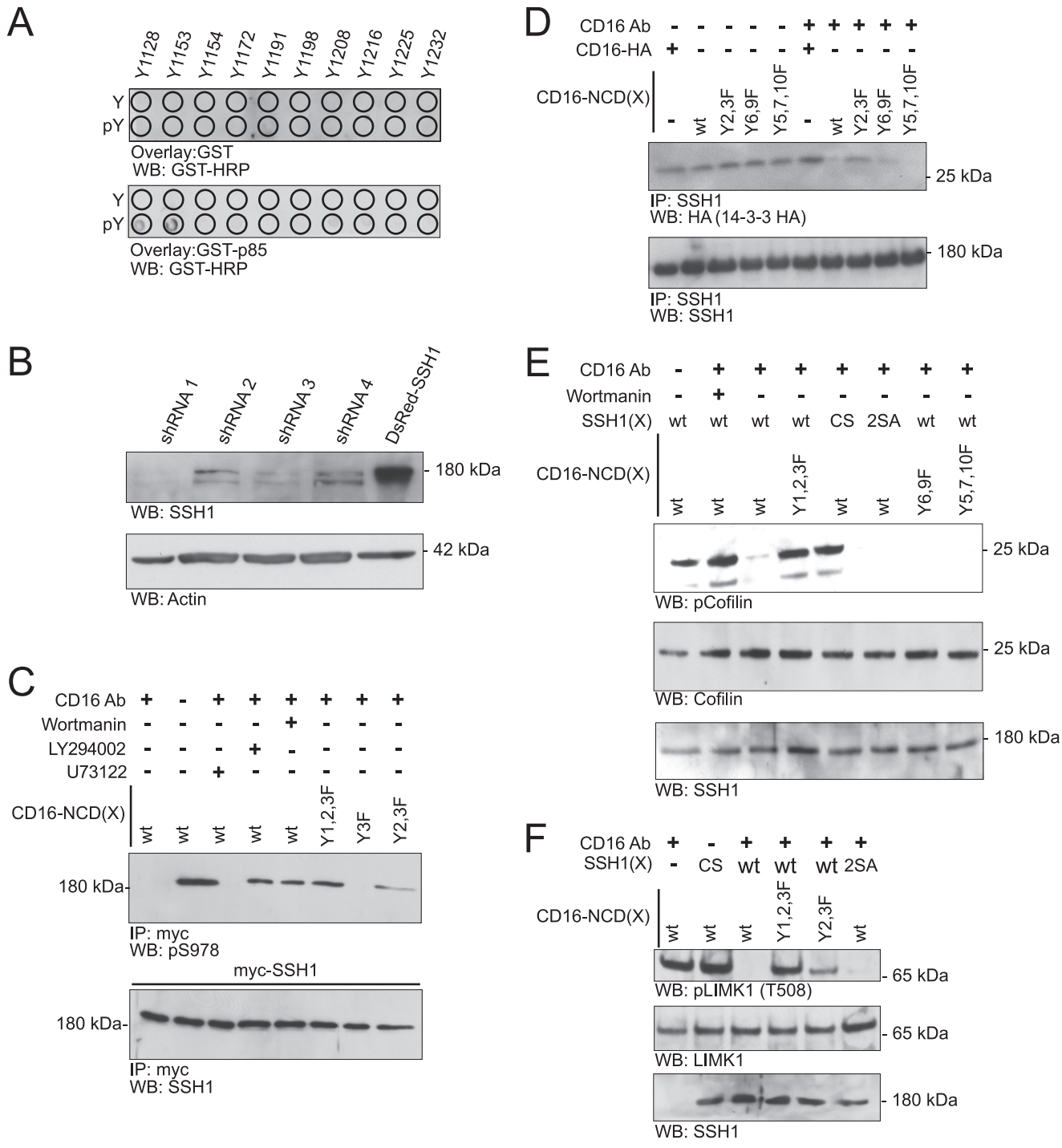

FIGURE 3. **Nephrin mediates cofilin dephosphorylation in a manner dependent on PI3K and Slingshot1.** *A*, GST-p85 overlay. Arrayed Nephrin oligopeptides synthesized with and without phosphorylated tyrosines were incubated with GST-p85 and then probed with horseradish peroxidase-conjugated anti-GST antibody. *B*, stable knockdown of SSH1. Human podocyte cell lines were produced in which four different small hairpin RNAs were stably expressed; cells incorporating shRNA 1 ($SSH1^{kd}$) were selected for additional studies. Western blot analysis examining SSH1 expression is shown. *C*, Nephrin ligation results in SSH1 dephosphorylation on its Ser^{978} residue. Human podocyte $SSH1^{kd}$ cells expressing Myc-SSH1 were co-transfected with plasmids encoding the indicated CD16-chimeric proteins. Where indicated, cells were pretreated with PI3K inhibitors LY294002 (*lane 4*) or wortmannin (*lane 5*). Phospholipase C inhibitor U73122 (*lane 3*) was used as a positive control because phospholipase activity is necessary for release of activated cofilin from a plasma membrane sequestered pool. Except where indicated, cells were treated with anti-CD16 antibody and anti-mouse IgG secondary antibody. Cell lysates were immunoprecipitated with Myc antibody and blotted with phospho-Ser^{978}-specific antibody. Lysates from the experiment were divided into two equal samples and loaded on two separate gels. *D*, Nephrin clustering abrogates association between SSH1 and 14-3-3. Human podocytes expressing HA-tagged 14-3-3ζ were co-transfected with the indicated plasmids encoding CD16-Nephrin or its tyrosine mutants or CD16-HA, and cells were treated as indicated with clustering antibody. CD16-HA represents a CD16/7 chimera in which the Nephrin cytoplasmic domain is replaced by an HA tag and serves as control. Cell lysates were immunoprecipitated using SSH1 antibody and blotted with indicated antibodies. *E*, Nephrin mediates cofilin Ser^3 dephosphorylation via PI3K and SSH1. Human podocyte $SSH1^{kd}$ cells expressing the indicated proteins were clustered using the CD16 antibody. Lysates were resolved using SDS-PAGE and blotted with indicated antibodies. *SSH1(CS)*, phosphatase-dead mutant; *SSH1(2SA)*, SSH1(S937A/S978A); *wt*, wild type SSH1. *F*, Nephrin-mediated SSH1 activation results in simultaneous LIMK1 dephosphorylation. $SSH1^{kd}$ cells expressing the indicated plasmids were clustered using the anti-CD16 antibody. Cell lysates were examined by Western blotting using the indicated antibodies. *IP*, immunoprecipitation; *WB*, Western blot; *WT*, wild type. Data are representative of three separate experiments.

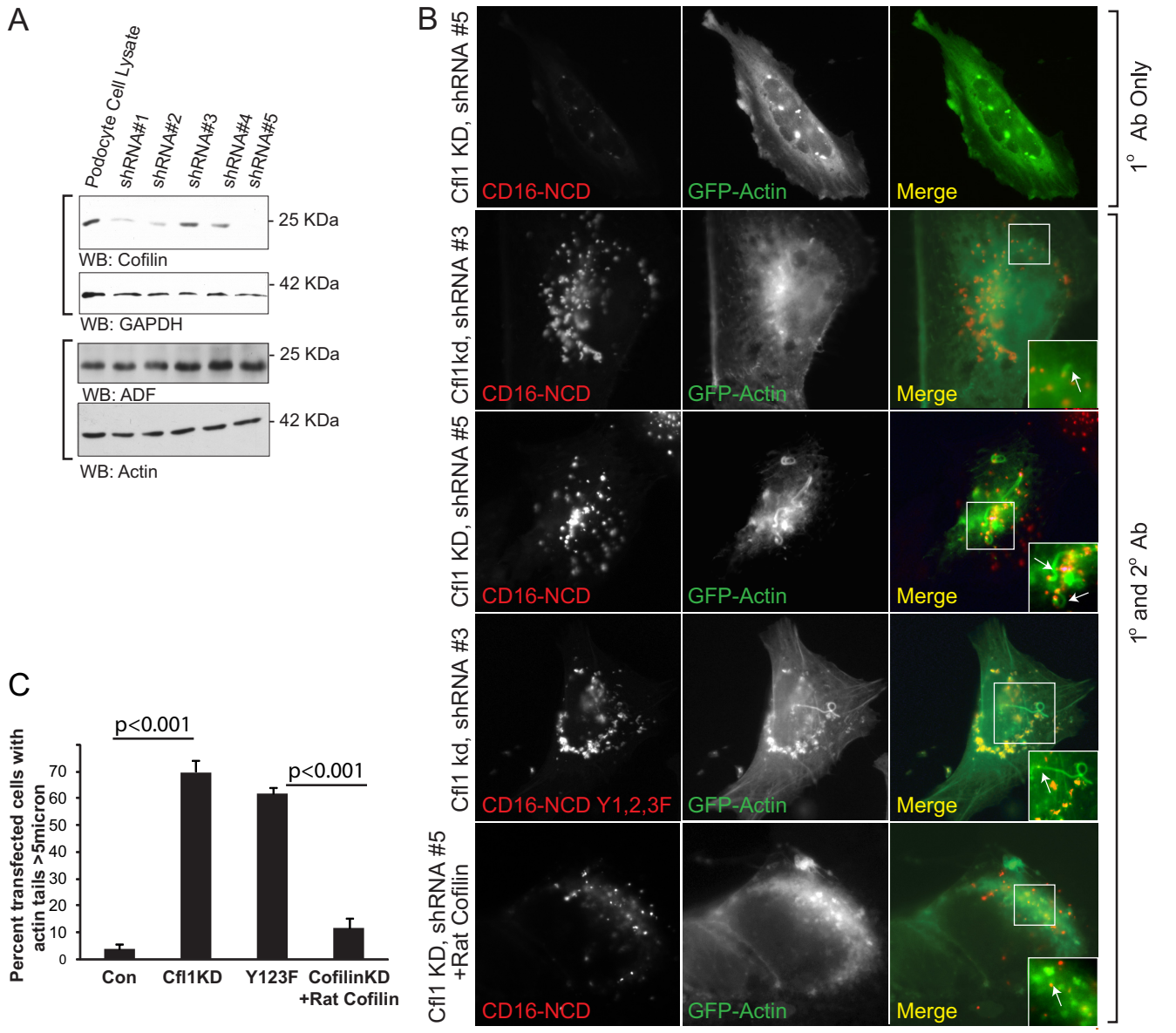

FIGURE 4. **Cofilin knockdown results in longer actin tails.** *A*, stable knockdown of cofilin-1. Human podocyte cell lines were produced in which five different small hairpin RNA oligonucleotides were stably expressed; cells incorporating shRNA ($Cfl1^{kd}$) were selected for additional study. After protein estimation, lysates were blotted for cofilin and ADF on two separate gels. Glyceraldehyde-3-phosphate dehydrogenase (*GAPDH*) and actin were used as loading controls for cofilin and ADF, respectively. *B*, human podocytes expressing the indicated plasmids were clustered as described and examined using confocal microscopy. The *arrows* indicate actin tails. Cells in the *top panel* were not treated with the secondary antibody. The rest of the *panels* show cells treated with both the primary anti-CD16 antibody and the anti-mouse IgG secondary antibody. *C*, percentage of cells with identifiable actin tails longer than 5 μm ($p < 0.001$). *Cfl1KD*, podocytes with stable knockdown using clone 5. As a control (*Con*), podocytes with infected with shRNA 3 was used. Image J software (National Institutes of Health) was used to determine the length of tail. Approximately 100 cells were analyzed in each condition. Data are representative of five separate experiments. *Error bars*, S.E.

An antagonist to the role of SSH1 in dephosphorylating and activating cofilin, LIMK inactivates cofilin catalytic activity by phosphorylating cofilin on Ser^3 (9). In keeping with the functional relationship between SSH1 and LIMK, activation of SSH1 also results in LIMK inactivation by dephosphorylation of LIMK(Thr^{508}) (48). Consistent with this previous observation, we observed that SSH1 is necessary for LIMK dephosphorylation upon Nephrin clustering (Fig. 3*F*).

Cofilin Knockdown Results in Longer Actin Tails—We hypothesized that Nephrin-induced actin polymerization would be altered in the absence of cofilin-1 because cofilin is necessary for actin depolymerization. A human podocyte cell line was prepared in which cofilin-1 was stably knocked down using lentivirus encoding shRNA (Fig. 4*A*). This cell line was transfected with CD16-Nephrin chimera and GFP-actin. Upon Nephrin activation, we observed exceptionally elongated actin tails in cofilin knockdown cells when compared with control (Fig. 4*B*). In cofilin knockdown cells, almost 70% of cells exhibited actin tails longer than 5 μm compared with less than 5% in control ($p < 0.001$) (Fig. 4*C*). Similarly, long actin tails were observed in cells expressing a CD16-Nephrin chimera with Y1F/Y2F/Y3F mutations that does not interact with p85 PI3K but retains the ability to induce actin filaments upon clustering. This phenotype was rescued upon expression of rat cofilin with

sequence dissimilarity to human cofilin. These results are reminiscent of results obtained previously by Mitchison and coworkers (49), who observed elongated actin filaments formed in *Xenopus* extract mixed with G-actin monomers and *Listeria* following immunodepletion of XAC (*Xenopus* ADF/cofilin). Taken together, these observations suggest a role for cofilin in Nephrin-mediated actin dynamics in podocytes.

Podocyte-specific Deletion of Cfl1 Results in Delayed Albuminuria and Podocyte Foot Process Spreading—To examine the function of cofilin-1 in true podocytes *in vivo*, we selectively deleted *Cfl1* from podocytes in the mouse. Using a Cre recombinase transgene driven by a podocyte-specific podocin promoter (39), exon 2 was deleted from *Cfl1* (Fig. 5*A*). Selective loss of cofilin-1 protein in podocytes was confirmed in kidney sections stained for cofilin and synaptopodin and imaged by fluorescence microscopy (Fig. 5*B*). The distribution of *Cfl1* genotypes obtained at 3 weeks postgestation from $Cfl1^{f/f} \times Cfl1^{f/+}$; $pod\text{-}cre^{Tg/+}$ crosses occurred at the expected Mendelian frequency. Mutant animals had a reduced life span with a median age at death of 9 months, when they exhibited large ascites and a scruffed appearance. At 1 month postgestation, mutant kidneys were not grossly different from control kidneys, and histology at this age was normal as assessed by scanning (Fig. 6*A*), transmission electron microscopy (Fig. 6*B*), and light microscopy (Fig. 6*D*). In particular, podocyte morphology in null kidneys examined at birth was normal. At 2 months postgestation, the mean urine albumin/creatinine ratio in mutant mice was not statistically different from control. Subsequently, mice deleted of *Cfl1* in podocytes developed increased albuminuria (Fig. 5, *C* and *D*). The rate of proteinuria accelerated modestly until 6 months and accelerated more rapidly thereafter. Although proteinuria was observed by 3 months in null mice, no alteration in podocyte morphology was detected by scanning EM at this time point. Indeed, discernable foot process spreading was not observed until 6 months, when the increased urinary albumin excretion rate was more exaggerated. These observations were corroborated using transmission electron microscopy to evaluate podocyte intercellular junction frequency (Fig. 6*C*). Alteration in podocyte density relative to wild type control was not observed at 3, 6, and 9 months (data not shown). No increase in scarring or inflammatory cell infiltrate in the interstitium was observed at 9 months in null mice (Fig. 6*D*). By 6 months of age, the mutant mice developed renal dysfunction as indicated by a rise in creatinine (Fig. 6*E*) when compared with control although there was no evidence of glomerular or interstitial scarring. These results suggested that cofilin-1 is necessary for the maintenance of podocyte morphology postgestation.

Given the known function of cofilin in cell motility, its role in early developmental events, and its signaling relationship with Nephrin, the observation that *Cfl1* null podocytes goes through normal morphogenesis was unanticipated. Because ADF is also expressed in podocytes and might complement cofilin-1 function, we examined the abundance of ADF protein in isolated glomeruli of *Cfl1* mutant mice. ADF abundance was increased in newborn *Cfl1* mutants relative to wild type control (Fig. 5*E*). Remarkably, ADF expression in mutants decreased with age. That albuminuria increased concomitantly with this decrease in ADF abundance suggested the hypothesis that increased ADF abundance transiently functionally complements deletion of cofilin-1 in mutant podocytes.

Cofilin-1 Is Necessary for Restoration of Podocyte Morphology following Injury—We hypothesized that cofilin-1 is necessary for foot process spreading in response to podocyte injury or that cofilin-1 is required for restoration of normal podocyte architecture during podocyte recovery. The protamine sulfate-heparin sulfate model was employed to investigate this hypothesis (50). In this model, perfusion of mouse kidneys with protamine sulfate results in foot process spreading, whereas subsequent perfusion with heparin sulfate results largely in restoration of normal podocyte morphology. Three-month-old littermates were chosen for study because at this age, mutant podocytes retained normal morphology. As anticipated, wild type podocyte foot processes exhibited lateral spreading following protamine sulfate perfusion and recovered normal morphology following additional perfusion with heparin sulfate (data not shown). Following 15-min protamine sulfate perfusion of *Cfl1* mutants, the podocyte foot processes exhibited a broadened and flattened morphology that was distinct from that observed following protamine perfusion of the wild type kidney (Fig. 7). In addition, protamine sulfate-treated mutant podocytes reproducibly ($n = 5$ of 5 experiments) developed long fine processes that projected from primary, secondary, and tertiary processes analogous to observations made in cell culture reported above. Furthermore, *Cfl1* mutant podocytes did not recover normal morphology following subsequent infusion of heparin sulfate. These observations are consistent with the conclusion that cofilin-1 is necessary for the typical response of podocyte cytoskeletal dynamics to podocyte perturbation with protamine sulfate.

DISCUSSION

The activated Nephrin-Neph1 receptor complex can induce actin filament nucleation and elongation at the plasma membrane by recruiting an actin polymerization complex in a tyrosine phosphorylation-dependent manner (23, 24, 35). Because this receptor complex is targeted to the podocyte intercellular junction during process development and because genetic deletion of Nephrin or Neph1 results in abnormal but not complete failure of podocyte process development, we hypothesize that beyond merely inducing actin polymerization, Nephrin and Neph1 participate in regulating actin architectural dynamics. In approaching this hypothesis, we reasoned that Nephrin might regulate enzymes involved in actin cytoskeletal remodeling during podocyte process development or during morphological changes that occur following podocyte injury or recovery (50–52). Consistent with this hypothesis, we report here that in cell culture, Nephrin activates the actin filament-severing enzyme cofilin via a PI3K-, SSH1-, 14-3-3-, and LIMK-dependent mechanism. Our additional observations that cofilin is activated following podocyte injury in a rat model, that cofilin is necessary for the typical morphological changes that occur following podocyte injury and during podocyte recovery, and that cofilin is necessary for maintaining podocyte structure with aging all support the conclusion that cofilin is a necessary component of the mechanisms that govern podocyte cytoskeletal

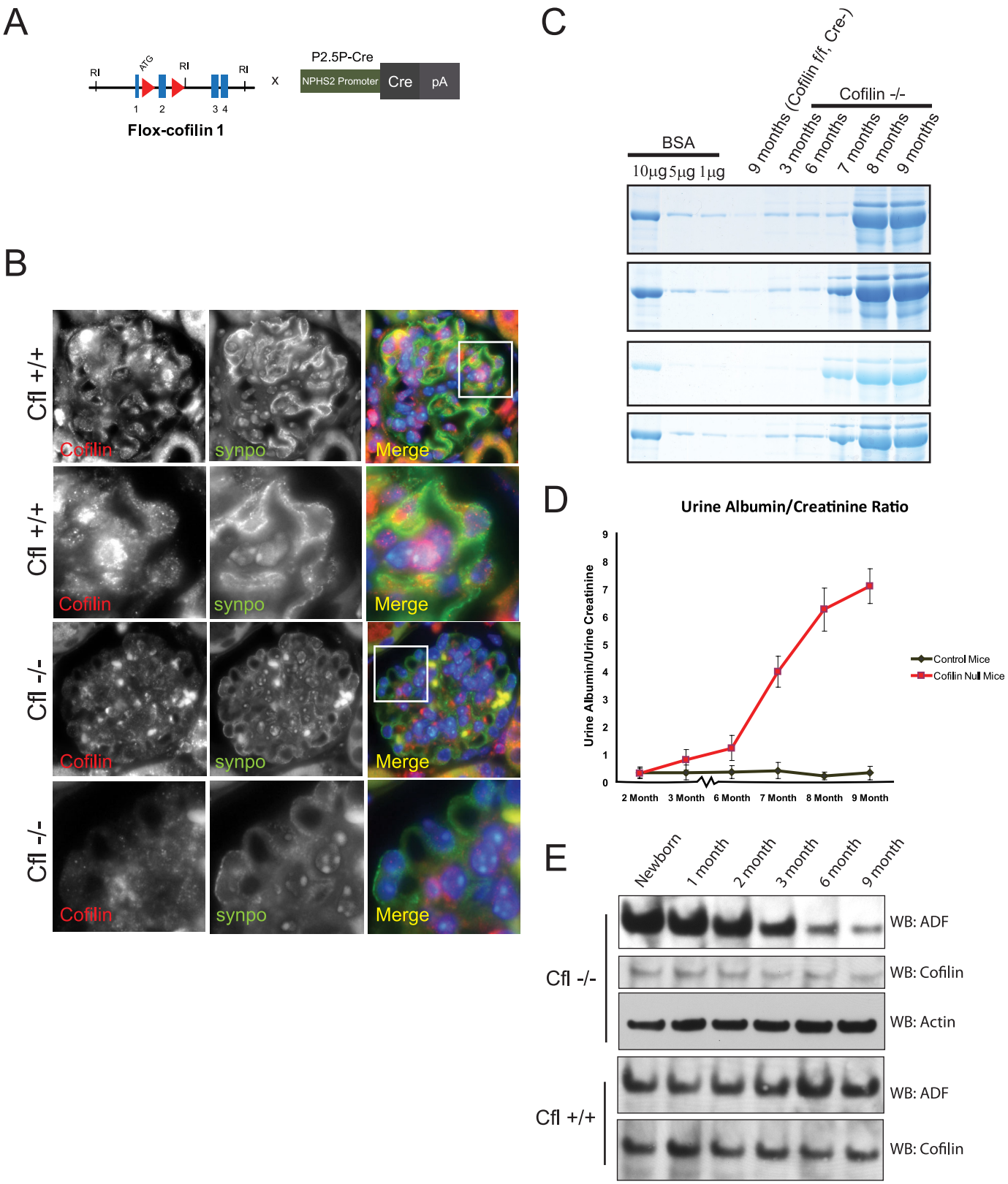

FIGURE 5. **Selective deletion of cofilin-1 in mouse podocyte.** *A*, cofilin-flox mice with *loxP* sites flanking exon 2 were bred with NPHS2-Cre mice to generate conditional knockdown of cofilin-1 in podocytes. *B*, double immunofluorescence of mouse kidney section. Paraffin-embedded mouse kidney sections from $Cfl1^{+/+}$ and $Cfl1^{-/-}$ mice were double-stained with cofilin-1 (*red*) and synaptopodin (*green*), showing podocyte specific deletion of Cfl1. Nuclei were stained with 4′,6-diamidino-2-phenylindole (*DAPI*). *Rows 2* and *4* show higher magnification of the area in the *white square*. *C*, urine protein. Urine was collected from the same mouse for the indicated times. The indicated concentrations of bovine serum albumin (*BSA*) were run as a quantitative measure. One microliter of urine was run in each *lane*. Gel was stained using SimplyBlue™ Safe Stain. Data from four different $Cfl1^{-/-}$ and $Cfl^{+/+}$ mice are shown. *D*, urine protein/creatinine ratio of $Cfl^{-/-}$ and $Cfl^{+/+}$ mice indicating the appearance of proteinuria by 3 months of age in $Cfl^{-/-}$ mice. *E*, ADF and cofilin expression in glomerular lysates for $Cfl1^{-/-}$ and $Cfl^{+/+}$ mice. Glomerular lysates from mouse kidneys were obtained at the indicated time points. Lysates were loaded equally after protein estimation. *WB*, Western blot. *Error bars*, S.E.

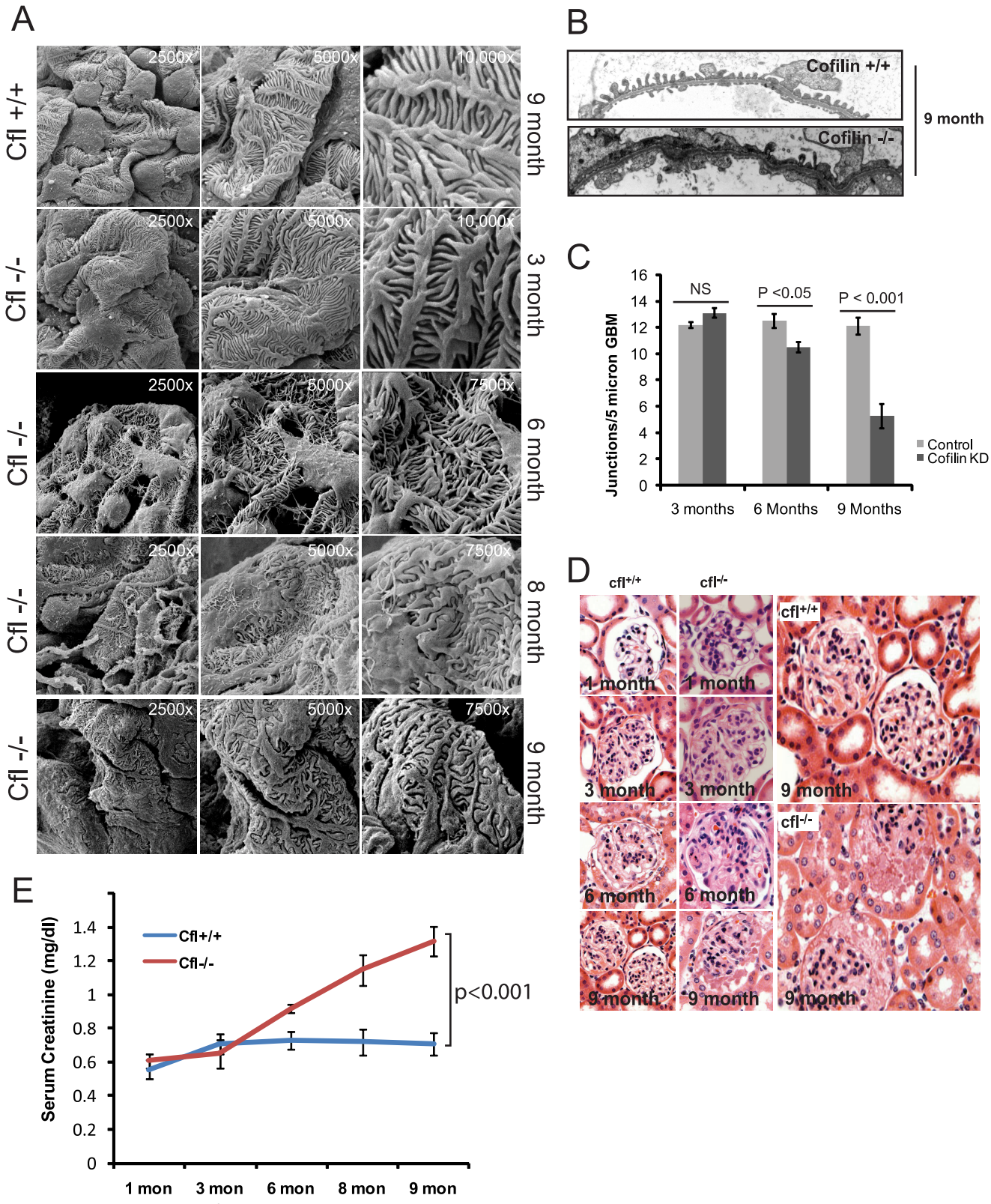

FIGURE 6. **Podocyte-specific *Cfl1*$^{-/-}$ mice develop foot process spreading by 8 months of age.** *A*, scanning EM of mouse kidney sections at the indicated postnatal age. There is evidence of foot process spreading by 8 months of age. There is evidence of fine finger-like projections from the podocyte cell bodies and processes at 6 months of age. *B*, transmission EM of *Cfl1*$^{-/-}$ and *Cfl*$^{+/+}$ mice at 9 months. *C*, slit diaphragm frequency in wild type and *Cfl*$^{-/-}$ mice at the indicated ages. *D*, histologically, hematoxylin and eosin staining of kidney sections from *Cfl1*$^{-/-}$ and *Cfl*$^{+/+}$ mice show no evidence of scarring even at 9 months of age, when the mouse are significantly proteinuric. *E*, serum creatinine concentration in mutant mice compared with control. *NS*, not significant. *Error bars*, S.E.

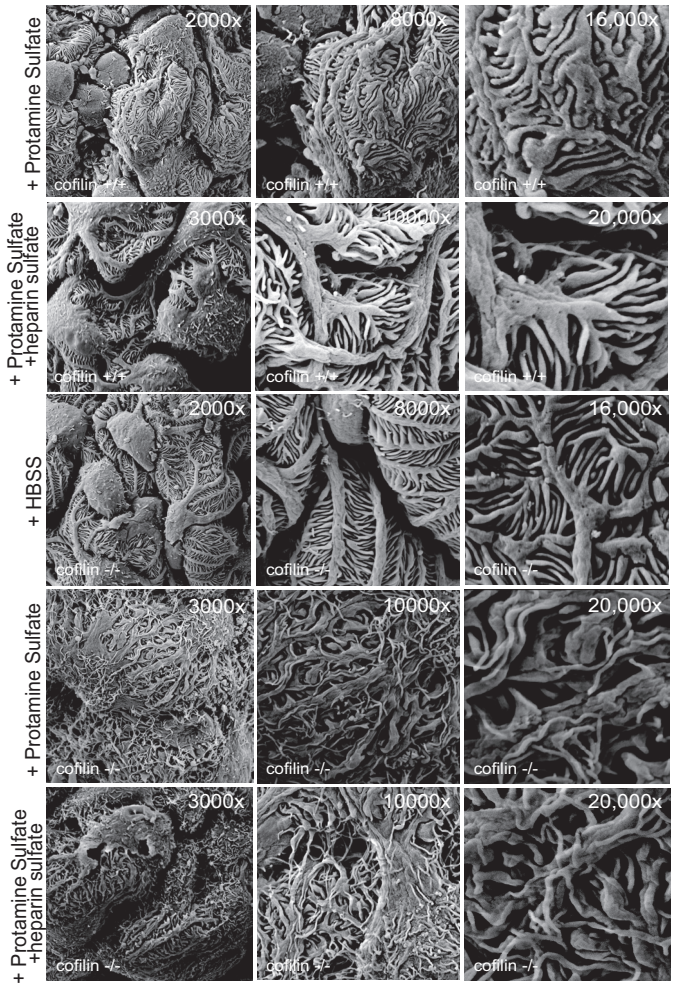

FIGURE 7. ***Cfl1* is necessary for restoration of podocyte morphology following injury with protamine sulfate.** Three-month-old *Cfl1*$^{-/-}$ and *Cfl*$^{+/+}$ mice were injected with HBSS and protamine sulfate where indicated. The *bottom panel* shows lack of recovery following heparin sulfate infusion. Data are representative of four or more mice for each experimental condition.

dynamics. Taken together, these results augment accumulating evidence that Nephrin participates in regulating actin dynamics in podocyte health and disease and suggest that this function is mediated in part via cofilin.

We were surprised to observe normal podocyte development in mouse podocytes deleted of cofilin, given the known functions of cofilin in determining actin cytoskeletal dynamics and cell polarity. Although this result suggests that cofilin is not necessary during podocyte morphogenesis, we cannot exclude the possibility that the obtained normal phenotype is due to an artifact of the experimental approach or to functional genetic complementation. Expression of Cre recombinase from the podocin promoter and DNA recombination takes place during the glomerular early capillary loop stage (39); ultimately, the loss of targeted protein expression following recombination depends on protein stability. Because deletion of some genes in floxed mice expressing the podocin-Cre transgene results in an abnormal podocyte developmental phenotype, it is not sufficient to explain the absence of a null phenotype in our experiments by delayed homologous recombination. Rather, loss of cofilin protein in mutant podocytes after the completion of initial cofilin-dependent developmental events might explain normal podocyte development if cofilin protein is relatively stable in this setting. Alternatively, we cannot discount the possibility that loss of cofilin in this model is complemented functionally by ADF. In their initial description of cofilin-1-deleted mice, Gurniak *et al.* (38) observed a severalfold increase in ADF protein abundance in embryonic tissue obtained from *Cfl1*$^{-/-}$ embryos relative to control. Consistent with that result, we noted increased abundance of ADF protein in podocyte-specific *Cfl1*$^{-/-}$ glomerular lysates. ADF abundance in null mice subsequently decreased to basal levels with aging, and it is noteworthy that this decline in ADF correlated with the onset of proteinuria at 3 months. Determination of whether this observation predicts that ADF functionally complements cofilin loss in this model will require additional study.

Delayed appearance of proteinuria and foot process effacement has been reported in patients with inherited mutations in actin-associated proteins *ACTN4, CD2ap*, and *INF2* (2, 4, 5). Like these human disease phenotypes, podocyte-specific cofilin null mice developed delayed onset proteinuria and changes in podocyte morphology. It is not clear why mutations in proteins that have been implicated in regulation of actin dynamics in cell culture models should result in a delayed glomerular phenotype. Perhaps these results suggest that mature podocyte foot processes are dynamic structures requiring changes in actin cytoskeleton to maintain healthy morphology, or perhaps these mutations result in early podocyte senescence. Podocyte loss beyond a yet undefined critical mass has been implicated as a precursor to development of scarring and proteinuria in rodent models of podocyte injury (43, 53). As *Cfl1* null mice aged, no difference in podocyte count per glomerulus was observed when cofilin null and wild type mice were compared, and mutant kidneys did not develop segmental sclerosis. Therefore, it is difficult to implicate early podocyte senescence and loss in the delayed phenotype observed here.

Podocyte morphology changes dramatically in response to podocyte protamine sulfate perfusion of the kidney; thereafter, podocyte shape is normalized by further perfusion with heparin sulfate. The observation that deletion of cofilin in podocytes perturbs these alterations was anticipated, indicating the necessity of cofilin during actin remodeling that presumably accompanies podocyte effacement. In addition to perturbing the ability of the podocyte to spread and recover following injury, protamine sulfate-perfused cofilin null podocytes developed unusual long fine processes projecting from primary, secondary, and tertiary processes. These changes might be described by the clinical renal pathologist as exaggerated "pseudovillous transformation" and are reminiscent of the exceptionally long actin tails observed in our cell culture experiments in which CD16-Nephrin was aggregated in cofilin-depleted podocytes. Both results in cell culture and results in the null mouse model are consistent with previous *in vitro* observations in which actin filament formation was dramatically elongated when *Xenopus* extract mixed with G-actin monomers and *Listeria monocytogenes* was depleted of XAC (49). Because cofilin promotes Arp2/3-mediated branching and formation of a broad lamellipodia-like leading edge by severing actin filaments into smaller fragments, it is possible that attenuation of this function in

podocytes depleted of cofilin promotes instead a filopodia-like structure created by actin filament elongation without branching.

Our observations also add to evidence suggesting that Nephrin plays an important role in regulating podocyte morphology by integrating multiple distinct signaling events that contribute to defining cytoskeletal architecture and dynamics. In addition to signaling via its interaction with the p85 subunit of PI3K to regulate cofilin-1 activity, Nephrin can signal via Nck- and phospholipase γ-dependent and potentially additional pathways to determine actin dynamics (23–25). Whether phosphotyrosine-dependent recruitment of these adaptor proteins and their associated protein complexes occurs simultaneously or whether these signaling events occur independently within specific functional contexts remains to be examined. Nevertheless, it is reasonable to speculate that multiple signaling pathways that either are induced by Nephrin-Neph1 activation or are activated concomitantly by other plasma membrane receptors are integrated to determine the unique morphology of the podocyte.

REFERENCES

1. Kestilä, M., Lenkkeri, U., Männikkö, M., Lamerdin, J., McCready, P., Putaala, H., Ruotsalainen, V., Morita, T., Nissinen, M., Herva, R., Kashtan, C. E., Peltonen, L., Holmberg, C., Olsen, A., and Tryggvason, K. (1998) *Mol. Cell* **1,** 575–582
2. Kim, J. M., Wu, H., Green, G., Winkler, C. A., Kopp, J. B., Miner, J. H., Unanue, E. R., and Shaw, A. S. (2003) *Science* **300,** 1298–1300
3. Winn, M. P., Conlon, P. J., Lynn, K. L., Farrington, M. K., Creazzo, T., Hawkins, A. F., Daskalakis, N., Kwan, S. Y., Ebersviller, S., Burchette, J. L., Pericak-Vance, M. A., Howell, D. N., Vance, J. M., and Rosenberg, P. B. (2005) *Science* **308,** 1801–1804
4. Brown, E. J., Schlöndorff, J. S., Becker, D. J., Tsukaguchi, H., Uscinski, A. L., Higgs, H. N., Henderson, J. M., Pollak, M. R., and Tonna, S. J. (2010) *Nat. Genet.* **42,** 72–76
5. Kaplan, J. M., Kim, S. H., North, K. N., Rennke, H., Correia, L. A., Tong, H. Q., Mathis, B. J., Rodríguez-Pérez, J. C., Allen, P. G., Beggs, A. H., and Pollak, M. R. (2000) *Nat. Genet.* **24,** 251–256
6. Pollak, M. R. (2003) *Semin. Nephrol.* **23,** 141–146
7. Ichetovkin, I., Grant, W., and Condeelis, J. (2002) *Curr. Biol.* **12,** 79–84
8. Hatanaka, H., Ogura, K., Moriyama, K., Ichikawa, S., Yahara, I., and Inagaki, F. (1996) *Cell* **85,** 1047–1055
9. Bamburg, J. R. (1999) *Annu. Rev. Cell Dev. Biol.* **15,** 185–230
10. DesMarais, V., Macaluso, F., Condeelis, J., and Bailly, M. (2004) *J. Cell Sci.* **117,** 3499–3510
11. Condeelis, J. (2001) *Trends Cell Biol.* **11,** 288–293
12. Nagata-Ohashi, K., Ohta, Y., Goto, K., Chiba, S., Mori, R., Nishita, M., Ohashi, K., Kousaka, K., Iwamatsu, A., Niwa, R., Uemura, T., and Mizuno, K. (2004) *J. Cell Biol.* **165,** 465–471
13. Huang, T. Y., DerMardirossian, C., and Bokoch, G. M. (2006) *Curr. Opin. Cell Biol.* **18,** 26–31
14. Bellenchi, G. C., Gurniak, C. B., Perlas, E., Middei, S., Ammassari-Teule, M., and Witke, W. (2007) *Genes Dev.* **21,** 2347–2357
15. Ghosh, M., Song, X., Mouneimne, G., Sidani, M., Lawrence, D. S., and Condeelis, J. S. (2004) *Science* **304,** 743–746
16. Moriyama, K., Iida, K., and Yahara, I. (1996) *Genes Cells* **1,** 73–86
17. Moriyama, K., and Yahara, I. (1999) *EMBO J.* **18,** 6752–6761
18. Zebda, N., Bernard, O., Bailly, M., Welti, S., Lawrence, D. S., and Condeelis, J. S. (2000) *J. Cell Biol.* **151,** 1119–1128
19. Bamburg, J. R., McGough, A., and Ono, S. (1999) *Trends Cell Biol.* **9,** 364–370
20. Mizuno, K., Okano, I., Ohashi, K., Nunoue, K., Kuma, K., Miyata, T., and Nakamura, T. (1994) *Oncogene* **9,** 1605–1612
21. Toshima, J., Toshima, J. Y., Amano, T., Yang, N., Narumiya, S., and Mizuno, K. (2001) *Mol. Biol. Cell* **12,** 1131–1145
22. Niwa, R., Nagata-Ohashi, K., Takeichi, M., Mizuno, K., and Uemura, T. (2002) *Cell* **108,** 233–246
23. Verma, R., Kovari, I., Soofi, A., Nihalani, D., Patrie, K., and Holzman, L. B. (2006) *J. Clin. Investig.* **116,** 1346–1359
24. Jones, N., Blasutig, I. M., Eremina, V., Ruston, J. M., Bladt, F., Li, H., Huang, H., Larose, L., Li, S. S., Takano, T., Quaggin, S. E., and Pawson, T. (2006) *Nature* **440,** 818–823
25. Harita, Y., Kurihara, H., Kosako, H., Tezuka, T., Sekine, T., Igarashi, T., Ohsawa, I., Ohta, S., and Hattori, S. (2009) *J. Biol. Chem.* **284,** 8951–8962
26. Zhu, J., Sun, N., Aoudjit, L., Li, H., Kawachi, H., Lemay, S., and Takano, T. (2008) *Kidney Int.* **73,** 556–566
27. Asanuma, K., Yanagida-Asanuma, E., Faul, C., Tomino, Y., Kim, K., and Mundel, P. (2006) *Nat. Cell Biol.* **8,** 485–491
28. Blasutig, I. M., New, L. A., Thanabalasuriar, A., Dayarathna, T. K., Goudreault, M., Quaggin, S. E., Li, S. S., Gruenheid, S., Jones, N., and Pawson, T. (2008) *Mol. Cell. Biol.* **28,** 2035–2046
29. Lehtonen, S., Ryan, J. J., Kudlicka, K., Iino, N., Zhou, H., and Farquhar, M. G. (2005) *Proc. Natl. Acad. Sci. U.S.A.* **102,** 9814–9819
30. Holzman, L. B., St John, P. L., Kovari, I. A., Verma, R., Holthofer, H., and Abrahamson, D. R. (1999) *Kidney Int.* **56,** 1481–1491
31. Lahdenperä, J., Kilpeläinen, P., Liu, X. L., Pikkarainen, T., Reponen, P., Ruotsalainen, V., and Tryggvason, K. (2003) *Kidney Int.* **64,** 404–413
32. Eiseler, T., Döppler, H., Yan, I. K., Kitatani, K., Mizuno, K., and Storz, P. (2009) *Nat. Cell Biol.* **11,** 545–556
33. Wary, K. K., Mariotti, A., Zurzolo, C., and Giancotti, F. G. (1998) *Cell* **94,** 625–634
34. Rivera, G. M., Briceño, C. A., Takeshima, F., Snapper, S. B., and Mayer, B. J. (2004) *Curr. Biol.* **14,** 11–22
35. Garg, P., Verma, R., Nihalani, D., Johnstone, D. B., and Holzman, L. B. (2007) *Mol. Cell. Biol.* **27,** 8698–8712
36. Saleem, M. A., O'Hare, M. J., Reiser, J., Coward, R. J., Inward, C. D., Farren, T., Xing, C. Y., Ni, L., Mathieson, P. W., and Mundel, P. (2002) *J. Am. Soc. Nephrol.* **13,** 630–638
37. Schiwek, D., Endlich, N., Holzman, L., Holthöfer, H., Kriz, W., and Endlich, K. (2004) *Kidney Int.* **66,** 91–101
38. Gurniak, C. B., Perlas, E., and Witke, W. (2005) *Dev. Biol.* **278,** 231–241
39. Moeller, M. J., Sanden, S. K., Soofi, A., Wiggins, R. C., and Holzman, L. B. (2003) *Genesis* **35,** 39–42
40. Moeller, M. J., Sanden, S. K., Soofi, A., Wiggins, R. C., and Holzman, L. B. (2002) *J. Am. Soc. Nephrol.* **13,** 1561–1567
41. Reiser, J., and Mundel, P. (2004) *J. Am. Soc. Nephrol.* **15,** 2246–2248
42. Verma, R., Wharram, B., Kovari, I., Kunkel, R., Nihalani, D., Wary, K. K., Wiggins, R. C., Killen, P., and Holzman, L. B. (2003) *J. Biol. Chem.* **278,** 20716–20723
43. Wharram, B. L., Goyal, M., Wiggins, J. E., Sanden, S. K., Hussain, S., Filipiak, W. E., Saunders, T. L., Dysko, R. C., Kohno, K., Holzman, L. B., and Wiggins, R. C. (2005) *J. Am. Soc. Nephrol.* **16,** 2941–2952
44. Wharram, B. L., Goyal, M., Gillespie, P. J., Wiggins, J. E., Kershaw, D. B., Holzman, L. B., Dysko, R. C., Saunders, T. L., Samuelson, L. C., and Wiggins, R. C. (2000) *J. Clin. Invest.* **106,** 1281–1290
45. Weibel, E. R., and Gomez, D. M. (1962) *J. Appl. Physiol.* **17,** 343–348
46. Bolender, R. P. (1979) *Anat. Rec.* **195,** 257–264
47. Nishita, M., Wang, Y., Tomizawa, C., Suzuki, A., Niwa, R., Uemura, T., and Mizuno, K. (2004) *J. Biol. Chem.* **279,** 7193–7198
48. Soosairajah, J., Maiti, S., Wiggan, O., Sarmiere, P., Moussi, N., Sarcevic, B., Sampath, R., Bamburg, J. R., and Bernard, O. (2005) *EMBO J.* **24,** 473–486
49. Rosenblatt, J., Agnew, B. J., Abe, H., Bamburg, J. R., and Mitchison, T. J. (1997) *J. Cell Biol.* **136,** 1323–1332
50. Reiser, J., von Gersdorff, G., Loos, M., Oh, J., Asanuma, K., Giardino, L., Rastaldi, M. P., Calvaresi, N., Watanabe, H., Schwarz, K., Faul, C., Kretzler, M., Davidson, A., Sugimoto, H., Kalluri, R., Sharpe, A. H., Kreidberg, J. A., and Mundel, P. (2004) *J. Clin. Investig.* **113,** 1390–1397
51. Lehtonen, S. (2008) *Kidney Int.* **73,** 903–905
52. Garg, P., Verma, R., and Holzman, L. B. (2007) *Nephron* **106,** e67–e72
53. Wiggins, R. C. (2007) *Kidney Int.* **71,** 1205–1214